ELSEVIER

Journal of Nuclear Materials 288 (2001) 87–91

journal of nuclear materials

www.elsevier.nl/locate/jnucmat

Thermal conductivity of U_3O_8 from 300 to 1100 K

C.G.S. Pillai, A.K. Dua, P. Raj *

Novel Materials and Structural Chemistry Division, Bhabha Atomic Research Centre, Mumbai 400 085, India

Received 9 June 2000; accepted 29 November 2000

Abstract

The thermal conductivity of orthorhombic α-U_3O_8 has been measured in air from 300 to 1100 K using an axial heat flow comparative set-up. The results show that the conductivity decreases monotonically with increasing temperature. The observed conductivity can be explained in terms of the phonon-defects and phonon–phonon interaction processes. It is also shown that the intrinsic thermal resistivity can be quantitatively explained by the modified Leibfried–Schlomann (LS) equation proposed by G.A. Slack (in: H. Ehrenreich, F. Seitz, D. Turnbull (Eds.), Solid State Physics, vol. 34, Academic Press, New York, 1979, p. 1).

1. Introduction

The thermal conductivity reports on U_3O_8 are very few and are limited to an upper temperature of 770 K [1–5]. Snyder and Kamm [1] and Schulz [2] studied the thermal conductivity values at various temperatures for low density U_3O_8 samples. Ross [3] and Schaekers and Lovell [4], on the other hand, reported the thermal conductivity for high density samples at 333 and 358 K, respectively. Noda and Naito [5] carried out the thermal conductivity measurements of U_3O_{8-z} for different O/U ratios, in the temperature range 200–750 K. This is quite unlike the case of UO_2, wherein a large number of investigations have been reported in the literature, which have been covered in a very recent exhaustive review article by Fink [6]. A comprehensive study on the activation energy of formation of U_3O_8 from UO_2, in a low temperature range, has been carried out by McEachern et al. [7]. From practical view point, this formation is very important, especially in the case of dry storage and ultimate disposal of used nuclear fuel. Similarly, in the case of a stray temperature excursion, there can be oxidation of UO_2 fuel resulting in the partial formation of U_3O_8. Modeling of the resultant heat transport in all these cases will require the information on the thermal conductivity of U_3O_8.

U_3O_{8-z} oxides are reported to exist in different crystalline forms [8–10]. The heat capacity (C_p) measurements on U_3O_{8-z} show lambda-type transitions and these transitions depend on the oxygen stoichiometry of the oxide [11,12]. In the present work, we report the thermal conductivity measurement of orthorhombic α-U_3O_8 in the temperature range 300–1100 K. From the measured thermal conductivity, phonon velocity and structural parameters, the phonon-defect and phonon–phonon contribution to thermal conductivity have been evaluated.

2. Experimental

The orthorhombic α-U_3O_8 used in this investigation was of nuclear purity obtained from Atomic Fuels Division, Bhabha Atomic Research Centre. Single-phase formation of the sample was ascertained by X-ray diffractometry, using monochromatic CuK_α radiation. Structural parameters, including the space group and atomic positions, were determined by Rietveld profile refinement of the X-ray diffraction pattern. Cylindrical blocks of 25 mm diameter and about 20 mm height required for thermal conductivity measurements were prepared by uniaxial cold compaction of the powder followed by sintering in air at 1373 K for 24 h and slow cooling thereafter. The bulk densities of the samples

* Corresponding author. Tel.: +91-22 550 5148; fax: +91-22 550 5151.

E-mail address: praj@apsara.barc.ernet.in (P. Raj).

0022-3115/01/$ - see front matter
PII: S0022-3115(00)00724-8

prepared were found to be 89% of the theoretical value. The microstructure of the sintered samples was examined by SEM using a Jeol 330 A microscope. The oxygen content of the samples used for the measurements was confirmed by the differential pulse polarographic technique [13]. The possible oxygen loss from the sample during thermal conductivity measurements was determined by thermogravimetry with the thermal analyzer model STA-409, Netzsch Gerätebau, GmbH, Germany.

The thermal conductivity was measured in air in the temperature range 300–1100 K by a steady-state axial heat flow comparative apparatus. In this arrangement, the sample was inserted between two identical reference materials (Pyroceram-9606 certified by NBS, USA) having the same diameter as that of the sample. An axial heat flow was established through this three-element stack by sandwiching it between a heat source and a heat sink and inserting the stack in a guard furnace consisting of four separate heaters. The thermal resistance at the interfaces of the sample and the reference was minimized by introducing a thin platinum foil between the two finely polished interfaces of each cylinder. The conductivity of the sample was determined from the thermal conductivity of the reference and the measured temperature gradient of the sample and the reference, when steady state was achieved. The accuracy of the measurement has been found to be within ±3%. More details of the apparatus have been described elsewhere [14]. The phonon or sound velocity in the sample at room temperature was measured using a Krautkrämer (Germany) ultrasonic thickness tester, model CL-204 and ultrasonic flow detector, model USIP-11.

3. Results

Fig. 1 shows the observed room temperature X-ray diffraction pattern of U_3O_8 along with the results of the Rietveld profile refinement analysis. It is found that the best fitting is obtained using the orthorhombic structure with space group Amm2 (No.38); the fitted structural parameters including atomic coordinates are listed in Table 1. These results are in very good agreement with the neutron diffraction data of Loopstra [15]. The polarographic measurement gave the O/U ratio of 2.667 ± 0.008 for the starting oxide. This value was found to be 2.665 ± 0.008 after completing the thermal conductivity measurements. Fig. 2 gives the base-line

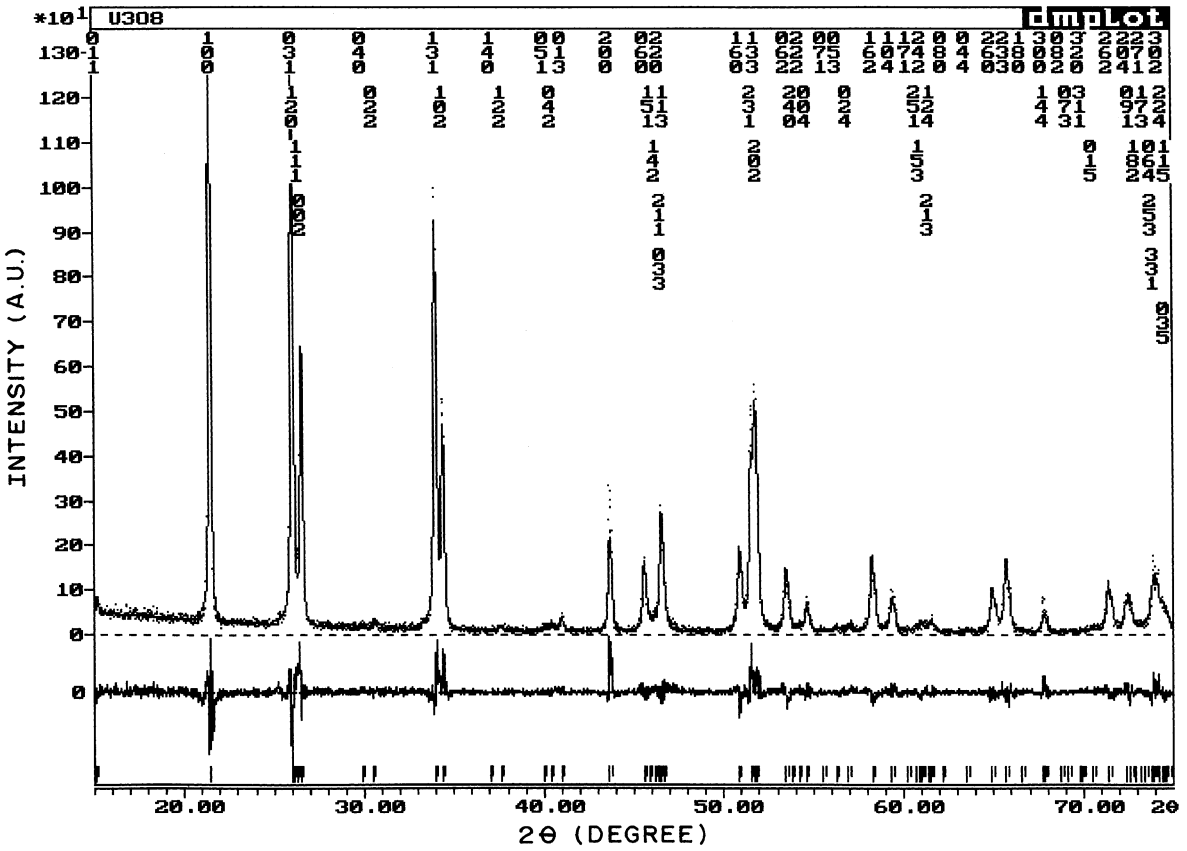

Fig. 1. X-ray diffraction pattern of U_3O_8 along with the Rietveld profile refinement analysis.

Table 1
Structural parameters of U_3O_8: orthorhombic space group Amm2 (No.38), $a = 4.1465$ (2) Å ; $b = 11.9471$ (6) Å ; $c = 6.7194$ (3) Å

Atom position		Fractional coordinates[a]		
		x	y	z
2 U(1)	in (a)	0	0	0.963
4 U(2)	in (d)	0	0.328	0
2 O(1)	in (b)	0.500	0	0.963
4 O(2)	in (e)	0.500	0.328	0
2 O(3)	in (a)	0	0	0.55
4 O(4)	in (d)	0	0.14	0.19
4 O(5)	in (d)	0	0.33	0.31

[a] The maximum uncertainty in U and O atoms positions are ±0.001 and ±0.01, respectively.

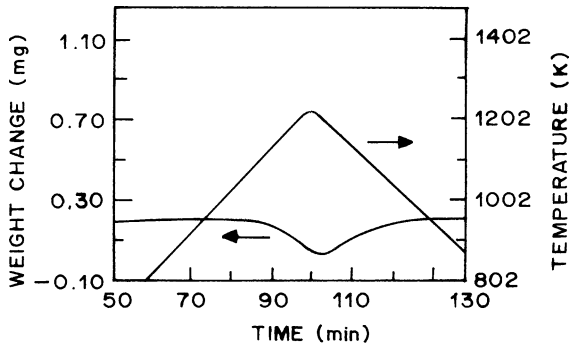

Fig. 2. Thermogravimetric curve of U_3O_8 (200.1 mg) in static air atmosphere; heating/cooling rate: 10 K/min; blank corrected.

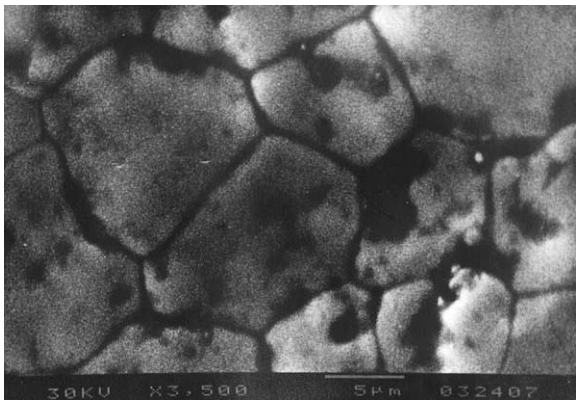

Fig. 3. Microstructure of U_3O_8.

corrected TG pattern obtained for the sample in both the heating and cooling cycles. From this figure, it is clear that there is no noticeable loss of oxygen up to 1100 K. However, on heating between 1100 and 1220 K the weight loss is 0.09%. This loss is fully recovered on cooling down to 1010 K. This corresponds to a variation of 0.047 in O/U ratio in agreement with earlier work [16]. Hence the oxygen content of the sample, which is subjected to repeated thermal cycling between 300 and 1100 K, will remain nearly the same. In order to get an idea about the nature of the porosity of the sample under investigation, its microstructure was examined by scanning electron microscopy. A typical micropattern is shown in Fig. 3. This examination suggested that the pores are largely spherical in shape and randomly distributed. Therefore, the observed thermal conductivity data were corrected using the following simplified equation [17]:

$$\lambda = \lambda_0(1 - P)^{3/2}, \tag{1}$$

where λ is the measured thermal conductivity, P is the fractional porosity and λ_0 is the conductivity corresponding to zero porosity. The conductivity corrected to 100% theoretical density ($P = 0$) is plotted as a function of temperature in Fig. 4. The literature data for thermal

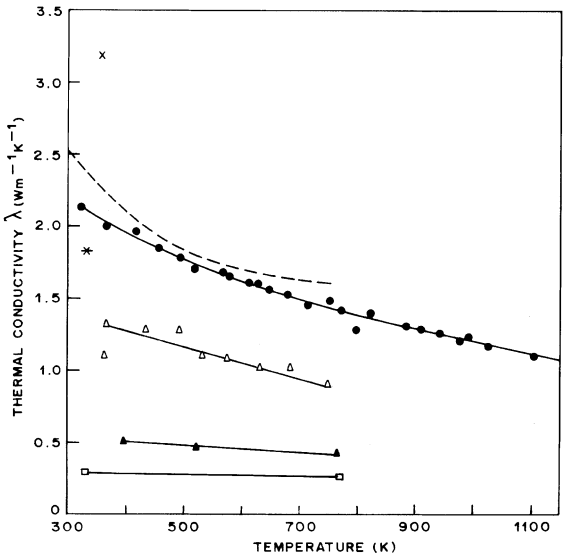

Fig. 4. Thermal conductivity of U_3O_8 corrected to 100% theoretical density as a function of temperature: (●) present data; (*) Ross [3]; (x) Schaekers and Lovell [4]; (- -) Noda and Naito [5]; (▲) pressed at 3 t/cm^2, (□) pressed at 7 kg/cm^2 ($P > 0$) Snyder and Kamm [1]; (△) ($P > 0.34$) Schulz [2].

conductivity values [3–5], recalculated for zero porosity correction using Eq. (1) have been included in Fig. 4. This corresponds to the following measurements: (i) at 333 K with O/U ratio of 2.66 and 96.2% theoretical density [3], (ii) at 358 K with 85% theoretical density [4], and (iii) temperature range 200–750 K with O/U ratio of 2.667 and 91.3% theoretical density [5]. The measured values for samples of 34% porosity by Schulz [2] and the samples pressed at 3 t/cm^2 and 7 kg/cm^2 by Snyder and Kamm [1] are also included in Fig. 4, without porosity correction. This is because Eq. (1) is not valid for 34% porosity samples, and Snyder and Kamm [1] have not given the density of the samples. The present measurements show that the conductivity decreases monotonically with increasing temperature. It may be noted that small lambda-type transitions at 483, 568 and 850 K with $\Delta H \approx 135$, 148 and 314 J mol^{-1}, respectively, reported in the C_p measurements of U_3O_8 [11], are not reflected in our thermal conductivity measurements. The sound velocity required for the calculations was measured and gave an average value of 3280 m/s.

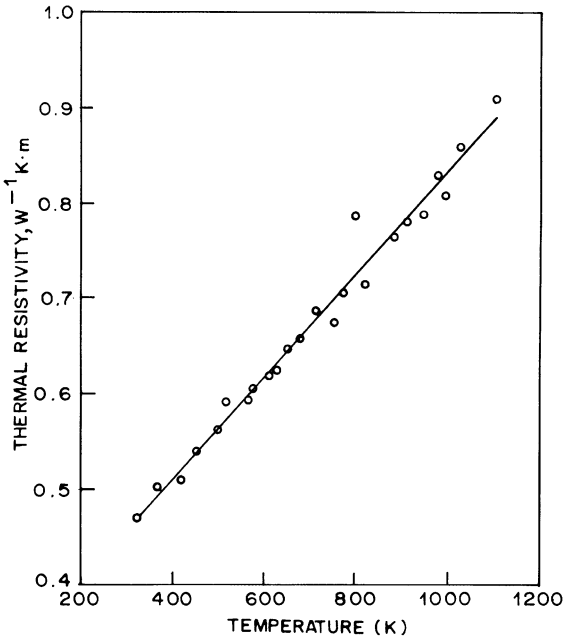

Fig. 5. Thermal resistivity of U_3O_8 as a function of temperature. The solid line is determined by fitting the thermal conductivity data to the relation $R = 1/\lambda = A + BT$, using the least squares method.

4. Discussion

The phonon contribution to thermal conductivity in typical ceramic materials can be expressed in the following form:

$$\lambda = 1/R = (A + BT)^{-1}, \tag{2}$$

where R is the thermal resistivity, T is the absolute temperature and A and B are constants. A gives the defect thermal resistivity and arises from the phonon interactions with lattice imperfections, impurities, isotopic or other mass differences as well as bulk defects such as grain boundaries, stacking faults in the sample. B gives a measure of the intrinsic phonon–phonon interactions. Fig. 5 shows that our thermal resistivity data fit very satisfactorily in the above form. The least-squares-fitted values of parameters A and B derived from our data from Fig. 5 are found to be $A = 29.3 \times 10^{-2}$ m KW^{-1} and $B = 5.39 \times 10^{-4}$ m W^{-1}. It is interesting to note that the observed conductivity of U_3O_8 is much less than that of UO_2 [18]. In the case of UO_2 the values of A and B are found to be 2.997×10^{-2} m KW^{-1} and 2.414×10^{-4} m W^{-1}, respectively [18]. The appreciably higher value of A of U_3O_8 shows that this oxide contains more defects compared with UO_2.

For a single-phase system, the intrinsic thermal resistivity, BT, can be estimated from basic material properties. Different theoretical expressions have been proposed in the literature [19–21], but the calculated values are found to be appreciably different from the experimental data in many cases [22]. We calculated the intrinsic thermal conductivity of UO_2 [18] and ThO_2 [23] using the Slack expression [24] obtained by modifying the Leibfried–Schlomann relation [20] and the results were found to be in good agreement with the experimental data. Similar calculations for U_3O_8 are described below.

The Slack expression for B is given as

$$1/B = (3.04 \times 10^{-6} \mathrm{MV}^{1/3}\theta_D^3)/(\mathrm{n}^{2/3}\gamma^2), \tag{3}$$

where M is the average atomic mass, V is the average atomic volume (in Å^3), θ_D is the Debye temperature, n is the number of atoms per molecule and γ is the Grüneisen parameter. The Debye temperature is calculated from the measured sound velocity v of U_3O_8 using the relation [25]

$$\theta_D = v(h/2\pi k)(V/6\pi^2)^{-1/3}, \tag{4}$$

where h and k are the Planck constant and Boltzmann constant, respectively. The calculated value of θ_D for U_3O_8 is found to be 395 K, using the average atomic volume of 15.13×10^{-30} m^3 obtained from the measured structural data (Table 1) and $v = 3280$ m/s. Using $\gamma = 2$ [24], $n = 11$ and other parameters as defined earlier, the calculated value of B is found to be 5.58×10^{-4} m W^{-1}. This value is in good agreement with that obtained from the experimental data of 5.39×10^{-4} m W^{-1}. The intrinsic parts of the conductivity calculated using the theoretical and experimental values of B are plotted in

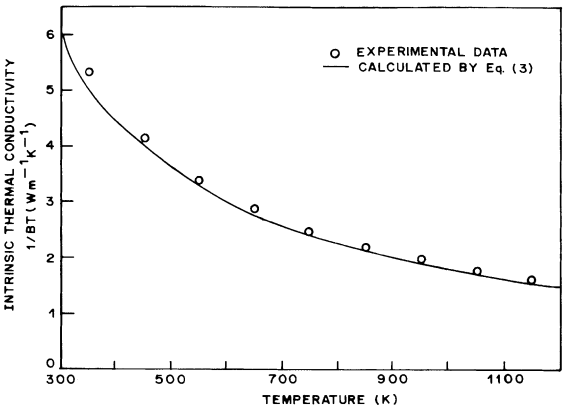

Fig. 6. Intrinsic phonon thermal conductivity of U_3O_8 obtained from experimental data and computed using Slack's expression (2), given as a function of temperature.

Fig. 6 as a function of temperature. A close agreement is found in this case. This agreement clearly shows that, as in the case of UO_2 and ThO_2, the above equation can be applied for U_3O_8 also.

5. Conclusions

The thermal conductivity of orthorhombic α-U_3O_8 in the temperature range 300–1100 K is found to be appreciably less than that of UO_2. The theoretical treatment shows that the expression of Slack obtained by the modified Leibfried–Schlomann equation can be applied for the quantitative estimation of the intrinsic phonon conductivity in this oxide. It is also concluded that thermal resistivity of U_3O_8 has large contribution from lattice defects.

Acknowledgements

Authors are grateful to Dr J.P. Mittal, Director, Chemistry and Isotope Group, BARC for his interest in this work. Thanks are also due to Dr P.V. Ravindran for the TG measurements; Sri. A.K. Bandyopadhyay, Atomic Fuels Division for the sound velocity measurements; Dr M.M. Palrecha and Ms Avanti Agnihotri, Analytical Chemistry Division for the O/U measurements, and Sri. M.P. Kuriakose for the help in the thermal conductivity measurements.

References

[1] T.M. Snyder, R.L. Kamm, USAEC Report, C-192, A-230 (1955).
[2] B. Schulz, Rev. Int. Htes. Temp. Refract. 12 (1975) 132.
[3] A.M. Ross, USAEC Report, CRFD-817, AECL-1096 (1960).
[4] J.M. Schaekers, G.H.B.Lovell, At. Energy Board Rep. S. Africa, PEL-195 (1969).
[5] Y. Noda, K. Naito, J. Nucl. Mater. 80 (1979) 102.
[6] J.K. Fink, J. Nucl. Mater. 279 (2000) 1.
[7] R.J. McEachern, J.W. Choi, M. Kolár, W. Long, P. Taylor, D.D. Wood, J. Nucl. Mater. 249 (1997) 58.
[8] G.C. Allen, N.R. Holmes, J. Nucl. Mater. 223 (1995) 231.
[9] P.E. Blackburn, J. Phys. Chem. 62 (1958) 897.
[10] R.J. Ackermann, A.T. Chang, J. Chem. Thermodyn. 5 (1973) 873.
[11] H. Inaba, H. Shimizu, K. Naito, J. Nucl. Mater. 64 (1977) 66.
[12] K. Naito, H. Inaba, S. Takahshi, J. Nucl. Mater. 110 (1982) 317.
[13] M.M. Palrecha, in: Proc. Nucl. Radiochem. Symp., Saha Insti. Nucl. Sci, Calcutta, 1997, 356.
[14] C.G.S. Pillai, A.M. George, Intl. J. Thermophys. 12 (1991) 701.
[15] B.O. Loopstra, Acta. Cryst. 17 (1964) 651.
[16] S.R. Dharwadkar, M.S. Chandrasekharaiah, M.D. Karkhanavala, J. Nucl. Mater. 71 (1978) 268.
[17] B. Schulz, High Temp. – High Press. 13 (1981) 649.
[18] C.G.S. Pillai, A.M. George, J. Nucl. Mater. 200 (1993) 78.
[19] P.G. Klemens, Proc. Phys. Soc. A 68 (1955) 1113.
[20] G. Leibfried, E. Schlomann, Nachr. Akad. Wiss. Göttingen Math. Phys. Kl. 4 (1954) 71.
[21] M. Roufosse, P.G. Klemens, Phys. Rev. B 7 (1973) 5379.
[22] C.G.S. Pillai, PhD thesis, Bombay University, 1987.
[23] C.G.S. Pillai, P. Raj, J. Nucl. Mater. 277 (2000) 116.
[24] G.A. Slack, in: H. Ehrenreich, F. Seitz, D. Turnbull (Eds.), Solid State Physics, vol. 34, Academic Press, New York, 1979, p. 1.
[25] V. Ambegaokar, Phys. Rev. 114 (1959) 488.